# Influence of the turbulence on a sensing path on the image of a focused laser beam

**V.M. Sazanovich and R.Sh. Tsvyk**

*Institute of Atmospheric Optics,*
*Siberian Branch of the Russian Academy of Sciences, Tomsk*

Received August 28, 2000

The influence of turbulence on formation of image of a laser beam by the receiving optical system was studied experimentally for the case of reflection from a mirror. The beam was focused on a reflector through both correlated (monostatic) and uncorrelated (bistatic) paths under conditions of strong intensity fluctuations. Intensity distributions in the plane of the reflector image were recorded and analyzed. It was shown that under certain conditions on the correlated path the intensity distribution has two scales, wide base (turbulent radius), and a narrow peak (coherent radius). The dependence of the radius of the beam image on the conditions of propagation and the diameter of the receiving objective was determined.

Space and time inhomogeneity of a random medium leads to blurring of the image of an object observed through it, and thus the information on fine details of an object is lost and the error in determination of its coordinates increases. In Refs. 1–7, it was shown that the quality of the object image observed formed in the location optical arrangement can be improved using the effects caused by the influence of correlation of waves propagating along the same paths. These effects include correlation of opposing waves (beams propagate through the same inhomogeneities in the forward and backward direction) and the effect of far correlations of the direct and reflected waves (separated opposing beams pass through the same inhomogeneities). The influence of correlation increases the coherence in a part of the reflected wave. The effect of far correlations was experimentally observed under laboratory conditions in Refs. 3 and 4. It was shown that the coherent component of light reflected from an object in a turbulent medium can be separated using the polarization properties of light, and the quality of an interference pattern can thus be improved significantly.

The increase of coherence in a reflected wave also gives rise to a narrow peak against the background of a turbulence-blurred spot in the intensity distribution in the focal plane of a receiving lens. Our experiments with the plane waves and finite-size reflectors[7] under conditions of strong intensity fluctuations ($\beta_0^2 = 1.23\, C_n^2 k^{7/6} L^{11/6} > 1$, where $C_n^2$ is the structure characteristic of the medium refractive index, $k = 2\pi/\lambda$ is the wave number, $L$ is the distance to the reflector), demonstrated that the amplitude of the narrow peak depends on the level of the turbulence in the medium. Part of the coherent component in the total energy of the beam has been estimated.

This paper presents the results of experimental studies of the influence of turbulence in the medium and the size of a receiving objective on the intensity distribution in the plane of image of a mirror reflector illuminated by a focused beam of coherent radiation. The measurement results on the correlated (the reflected beam propagates strictly backwards) and uncorrelated (the beam reflected from an object is separated from the direct one so that the mutual influence of correlation effects is almost excluded) paths are compared.

The experiments were conducted under laboratory conditions with a setup modeling the conditions of developed convection above a heated surface. The geometry of the experiment is shown in Fig. 1.

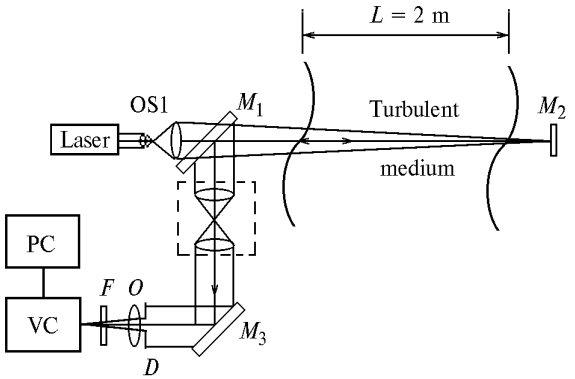


**Fig. 1.** Geometry of the experiment.

A He–Ne laser emitting at the wavelength $\lambda = 0.63$ μm was used as a source of radiation. A wave with the initial Gauss intensity distribution and the effective radius $a = 0.7$ cm and focused on the object was formed with an OS1 optical system (the mirror $M_2$ did not limit beam wandering). The Fresnel parameter of the emitter was $\Omega = ka^2/L = 70$, and the beam passed the turbulent layer three times, so the total path length was $L = 7$ m. In the monostatic optical arrangement, the beam reflected from the $M_2$ mirror passed through the same path in the forward and backward directions. Then, with the beam-splitting plate $M_1$ and the mirror $M_3$, it was directed to the

0235-6880/00/10 834-04 $02.00 

receiving telescope $O$ through a changeable diaphragm $D$ and an interference filter $F$. The size of the diaphragms varied from 0.6 to 7.5 times the Fresnel zones ($\sqrt{\lambda L}$). For analyzing the effect of correlation of opposing waves on the object image, the telescope was set strictly in the source plane, and the axes of the telescope and the source were aligned. To observe an object through an uncorrelated path of the doubled length, we changed the arrangement of the reflecting elements ($M_2$, $M_3$, and additional mirrors) providing for beam propagation in the forward and backward directions along different paths.

The studies were conducted under conditions of strong intensity fluctuations, at which the parameter $\beta_0^2$ characterizing the conditions of propagation through the atmosphere exceeded unity ($\beta_0^2 > 1$). The level of turbulence on the path was determined by measuring fluctuations of the arrival angles of a plane wave. For this purpose, we have organized an additional path without reflection (path length of 2 m in the medium) with a separate source and an optical system forming a quasi-plane wave with the Fresnel number $\Omega_1 = 35$. The level of turbulence on the propagation path could be varied by changing the temperature of the heated surface or the height of the beam propagation over this surface. In this experiment, only the height of propagation was varied to change the turbulent conditions. The laser beams of the main and additional paths propagated at the same height. The level of turbulence and the size of the image were measured simultaneously. The structure constant of the refractive index of the medium $C_n^2$ as a function of height $h$ above the heated surface can be found, for example, in Ref. 6.

Object images were recorded with a video camera (VC) set in the object's image plane and stored in a computer with the accumulation of 200 frames (during 6 min). The image size was 256×256 pixels, and the spatial resolution of the system "camera+computer" was about 27 μm.

To determine parameters of the intensity distribution, the horizontal ($X$) and vertical ($Y$) cross sections of the image were taken. These cross sections were obtained by averaging over two rows ($X$ axis) and columns ($Y$ axis) including the maximum of the intensity distribution. Then the amplitude of the intensity distribution was normalized to the maximum value equal to $A_1 + A_2$, and the parameters $A$, $a$, and $x_0$ of an exponent $A \exp[-((x - x_0)/a)^2]$ or the sum of two exponents $A_1 \exp[-((x - x_{01})/a_1)^2] + A_2 [-((x - x_{02})/a_2)^2]$ most accurately describing this distribution were fitted for every intensity distribution measured. This processing technique allows determination of the amplitude ratio and effective scales of a distribution to be done without measuring the absolute values of intensity. Figure 2 shows an example of the image and its intensity distributions in the horizontal and vertical cross sections.

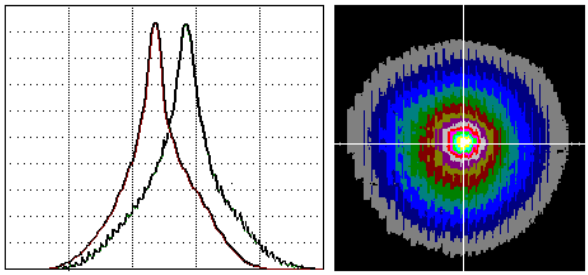

**Fig. 2.** Example of the intensity distribution recorded.

Let us consider the results obtained on the uncorrelated path. The beam is focused at a reflector installed at the same distance from the source and the receiver. In our experiments in a homogenous medium, geometrical optics gives 0.1 mm for the size of the spot on the reflector. This value corresponds to the Fresnel parameter of the reflector $\Omega_r = ka^2/L = 1.4 \cdot 10^{-2}$. Consequently, the reflected wave can be considered as a spherical one. For the spherical wave, the minimum size of the image of a light source taken through the turbulent atmosphere depends[1] not only on the scale of diffraction on the receiving lens, but also on the coherence length of the wave $\rho_s$:

$$a_{t\,min} \approx (4/\rho_s + 4/D_t^2)^{1/2}/[k(F_t^{-1} - L^{-1})], \quad (1)$$

where $F_t$ and $D_t$ are the focal length of the receiving objective and the diameter of the entrance diaphragm, respectively; $L$ is the distance from the reflector to the receiving optical system; $\rho_s = (0.55 C_n^2 k^2 L)^{-3/5}$ is the coherence length of the spherical wave. The dependence on $\rho_s$ leads to the image blurring as compared to a homogeneous medium. In the region of strong intensity fluctuations, the size $a_{t\,min}$ depends only on the turbulence intensity along the path and does not depend on the diameter of the receiving aperture:

$$a_{t\,min} \approx 2F_t/(k\rho_s). \quad (2)$$

Figure 3 shows the determined minimum size of the source image on the uncorrelated path at three values of the level of turbulence, $\beta_0^2$, on the path and different receiving apertures.

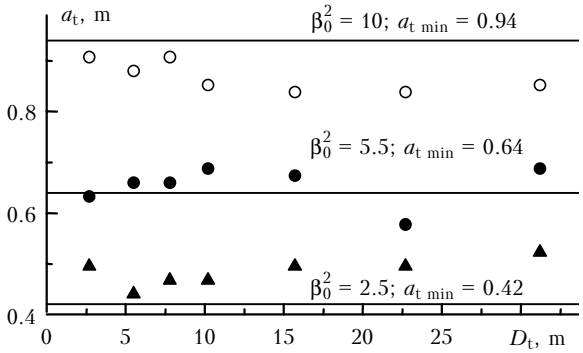


**Fig. 3.** Dependence of the beam radius $a_t$ on the diameter of the receiving objective $D_t$ on the uncorrelated path. The straight lines correspond to the minimum radius calculated by Eq. (2).

Under these conditions, the functions of intensity distribution have a single scale and are well described by the Gaussian distribution. It is seen from the figure that the minimum size of the object image is independent of the diameter of the receiving optical system. The scatter of data is mostly determined by variations of the parameter $\beta_0^2$, which was measured accurate to 10–15%, and only its mean values for measurement series are given in the figure. The straight lines in the figure show the minimum size of the image calculated by Eq. (2) for the case of strong intensity fluctuations. In this case, $\beta_0^2$ was determined for a path of the length $L$. Thus, focusing the beam on the path center has led to situation that the focusing point became a source of a spherical wave, whose parameters corresponded to propagation along the path of length $L$ to the reflector. This means that the optical wave after reflection partially "forgets" the influence of the path section from the source to the reflector.

Different situation is observed on the correlated path. In this case, the intensity distribution in the object's image plane depends on both the diameter of the receiving aperture and the level of turbulence along the path. In our experiment, the least diameter of the receiving aperture of 2.7 mm, corresponding to $0.6\sqrt{\lambda L}$, gives the intensity distribution close to the single-scale one at all $\beta_0^2$ values used in the experiment. The mean size of the image in this case is 1.5–2 times less than that on the uncorrelated path at the same values of $\beta_0^2$. At $\beta_0^2 \approx 2.5$ it is comparable with the diffraction-limited size of the image.

The deviation from the single-scale distribution becomes noticeable at the receiver aperture greater than $\sqrt{\lambda L}$. Against the background of a wide turbulence-blurred image of radius $a_t$, a narrower peak appears in the central part of the spot with the radius $a_d$. Thus, at small apertures, a narrow beam propagating near the axis and having high coherence forms the image. The radius of the narrow peak increases with the growth of $\beta_0^2$ more slowly than $1/\rho_s$ does.

Figure 4 shows the values of the turbulent (wide base, Fig. 4*a*) and coherent (narrow peak, Fig. 4*b*) lengths of the intensity distribution under different experimental conditions. It is seen from Fig. 4 that the beam radius increased by turbulence grows slowly with increasing diameter of the receiving aperture at $\beta_0^2 = 5.5$ and 10. This effect can likely be explained by changes in the image focusing at large values of $\beta_0^2$, since the plane of analysis was constant in the process of experiment. The coherent length decreases with increasing diaphragm and practically does not depend on the level of turbulence. The solid curve in Fig. 4*b* shows the diffraction-limited size of the image ($a_d = 1.22\lambda F_t/D_t$) calculated for the apertures used. The measured values of the radius well fit this curve.

The amplitudes of distribution of the turbulent and diffraction scales are shown in Fig. 5. The highest amplitude of the narrow peak characterizes the distributions corresponding to small diaphragms. As the aperture of the entrance objective increases, the amplitude and the radius of the narrow peak decrease, the narrow peak becomes more pronounced and noticeable against the background of a wide turbulent spot, but its contribution to the total energy of the beam in the image plane decreases.

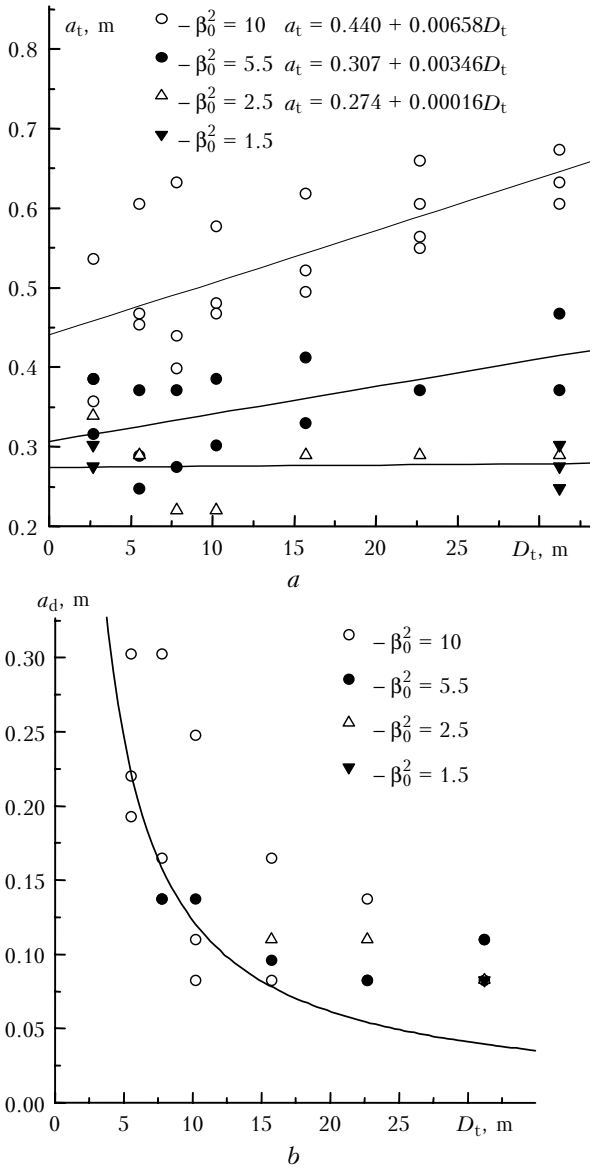


**Fig. 4.** Radius of turbulent $a_t$ (*a*) and diffraction-limited $a_d$ (*b*) parts of the beam on the correlated path as a function of the receiving objective diameter $D_t$ at different level of turbulence $\beta_0^2$.

The measured size of the turbulent image of the object for the correlated and uncorrelated paths was compared with the size calculated by equations from Ref. 1 that take into account the parameters of the beam and the conditions of propagation. Figure 6 shows the results of this comparison for one diaphragm and different $\beta_0^2$. The measured values for the both paths lie between the calculated ones for the distances $L$ and $2L$.

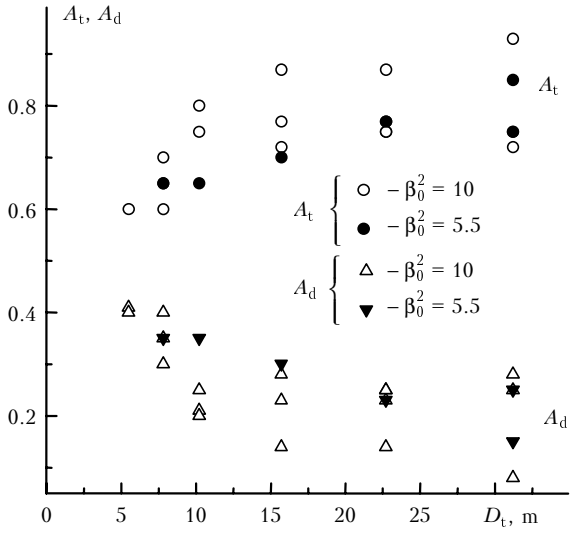


**Fig. 5.** Amplitude of turbulent $A_t$ and diffraction $A_d$ parts of the beam as a function of the receiving objective diameter $D_t$ at different levels of turbulence $\beta_0^2$.

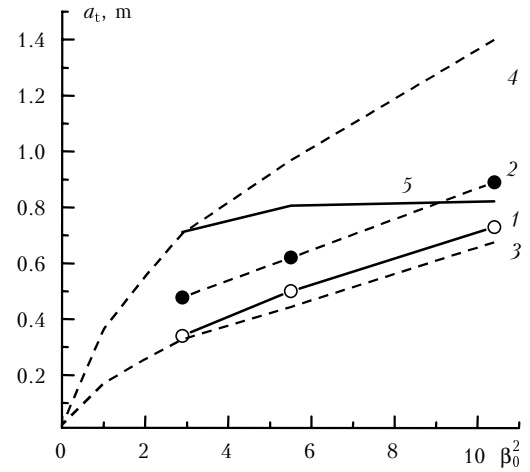


**Fig. 6.** Comparison of calculated and measured values of the turbulent radius of the image $a_t$ for the receiving objective $D_t = 32$ mm in diameter: correlated and uncorrelated paths (*1* and *2*), calculated radius for the path of length $L$ and $2L$ (*3* and *4*), ratio of the radii on correlated and uncorrelated paths (*5*).

It should be noted that the radius of the image for the case of uncorrelated path is roughly 1.5 times less than the calculated one for the $2L$-long path in contrast to the case of reflection of a wide collimated beam, in which the calculated and experimental data were close to each other.[7] The radius of image for the correlated path is 15–25% less than that on the uncorrelated one; at $\beta_0^2 > 5$ their ratio is independent of $\beta_0^2$.

Figure 7 shows the results of comparison of the turbulent radii of the image on the correlated $a_{t.c}$ and uncorrelated $a_{t.u}$ paths under different propagation conditions and receiving objective diameters. The straight line in the figure is calculated by the least-squares method ($r$ is the correlation coefficient). The high correlation between the turbulent radii of the beam is obvious, but the beam radius on the correlated path is always smaller than that on the uncorrelated one.

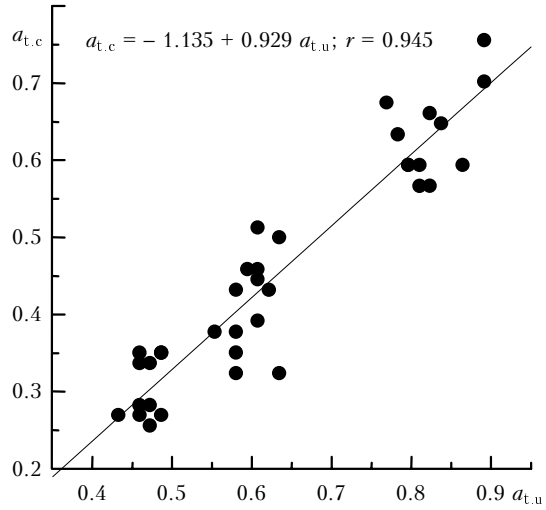


**Fig. 7.** Comparison of turbulent radii of the image on the correlated $a_{t.c}$ and uncorrelated $a_{t.u}$ paths.

## Conclusions

Comparison of the experimental results on formation of the image of a mirror reflector illuminated by a focused laser beam propagating under conditions of strong intensity fluctuations along correlated (monostatic) and uncorrelated (bistatic) paths allowed the following conclusions:

– under certain conditions on the correlated path, the intensity distribution has two characteristic scales: wide spot caused by turbulent blurring and the narrow (coherent) spot with the radius close to the diffraction-limited one calculated for the diameter of the receiving objective;

– in all measurements, the turbulent size of the beam on the correlated path is roughly 15–25% less than that on the uncorrelated path; this leads to roughly 1.5 times increase in the maximum intensity on the axis;

– on the uncorrelated path, the image radius is roughly 1.5 times less than that calculated for the path of $2L$ length, but larger than that for the path of the length $L$; it is independent of the receiving objective diameter and close to the limiting turbulence-dependent radius $a_{t\,min} \approx 2F_t/(k\rho_s)$ in the turbulent medium on the path of the length $L$.

### References

1. V.E. Zuev, V.A. Banakh, and V.V. Pokasov, *Optics of Turbulent Atmosphere* (Gidrometeoizdat, Leningrad, 1988), 270 pp.
2. A.B. Krupnik and A.I. Saichev, Izv. Vyssh. Uchebn. Zaved., Ser. Radiofizika **XXIV**, No. 10, 1234–1239 (1981).
3. A.N. Bogoturov, A.S. Gurvich, Y.C. Dainty, et al., Opt. Lett. **17**, No. 10, 757–759 (1992).
4. A.N. Bogoturov, A.A.D. Canas, Y.C. Dainty, et al., Opt. Commun. **87**, 1–4 (1992).
5. V.A. Banakh and B.N. Chen, Atmos. Oceanic Opt. **7**, No. 11–12, 827–830 (1994).
6. V.A. Banakh, V.M. Sazanovich, R.Sh. Tsvyk, and B.N. Chen, Atmos. Oceanic Opt. **9**, No. 12, 1033–1036 (1996).
7. V.A. Banakh, V.M. Sazanovich, R.Sh. Tsvyk, and B.N. Chen, Atmos. Oceanic Opt. **11**, No. 10, 910–913 (1998).